EFFECTIVE ERROR ESTIMATION FROM CONTINUOUS, BOUNDARY ADMISSIBLE ESTIMATED STRESS FIELDS

A.C.A. Ramsay† and E.A.W. Maunder‡

† Departamento de Engenharia Civil, Instituto Superior Técnico, Universidade Técnica de Lisboa, Avenida Rovisco Pais, 1096 Lisboa CODEX, Portugal.

‡ School of Engineering, University of Exeter, North Park Road, Exeter, Devon, EX4 4QF, England.

(Sent March 1995)

Abstract - Effective error estimation in plane stress linear-elastic problems using continuous, boundary admissible estimated stress fields is discussed. An error estimator based on continuous estimated stress fields achieved by interpolating from unique nodal stresses over the element with the element shape functions and in which the static boundary conditions are applied is introduced. The unique nodal stresses are achieved by the computationally cheap approach of simple nodal averaging of the finite element stresses at a common node. Results for this error estimator on a number of familiar benchmark problems are presented for the standard four-noded Lagrangian displacement element, and compared with those of other error estimators currently under research.

INTRODUCTION

Application of the standard displacement finite element method to problems in stress analysis results in a solution which, whilst satisfying compatibility[1] and the constitutive relations for the material(s), generally violates equilibrium. This lack of equilibrium manifests itself in:

1. a lack of internal equilibrium,
2. a lack of interface equilibrium, and
3. a lack of equilibrium on the static boundary.

Of these three *error indicators* the lack of interface equilibrium may be considered the most readily observed through consideration of the continuity, or otherwise, of the direct stress normal to, and the shear stress tangential to an element interface. Traditionally this error indicator has served the engineer in highlighting areas of the mesh for which the finite element approximation is insufficient.

Error indicators such as this, although indicating the presence of error, do little to help the engineer actually to quantify the error. More recently, however, *error estimators* which can quantify the error in the form of a single number known as an *error measure* have become popular areas of research. The error measure represents the total error in a single element and thus can be used to indicate the distribution of error within a mesh. Alternatively, the elemental error measures may be summed to give an error measure for the entire mesh. The motivation behind such research lies in the need for effective error estimation in the *self-adaptive procedures* which are, increasingly, being implemented in commercial finite element software codes.

Error estimators currently under research can be divided into the following three categories:

1. those that quantify the error directly in terms of residual quantities [1,2,3,4],
2. those that quantify the error indirectly through the construct of a stress field that is continuous [4,5,6,7], and a better estimate of the true stress field, and
3. those that quantify the error indirectly through the construct of stress field that is statically admissible [8,9,10,11], and a better estimate of the true stress field.

Recent research [16,17,20] has demonstrated that the effectivity of error estimators based on estimated stress fields that are continuous can be significantly enhanced through the simple expedient of 'applying the static boundary conditions' to the estimated stress field. Such

[1]Note: this assumes that the kinematic boundary conditions are satisfied exactly.

estimated stress fields could then be termed *boundary admissible*. In this paper a simple error estimator utilising an estimated stress field which is both continuous and boundary admissible is considered.

The research detailed in this paper considers the problem of plane linear elasticity. In particular, the performance of error estimators for the standard four-noded Lagrangian displacement element are examined.

ERROR MEASURES

The philosophy of error estimation given here is presented in terms of familiar strain energy quantities rather than the, perhaps, less familiar energy norm quantities generally used in the literature. This approach was developed in [15] with the aim of making the subject of error estimation more approachable to the practising engineer - the people who will ultimately use such concepts.

The finite element method results in a finite element stress field $\{\sigma_h\}$ as an approximation to the true stress field $\{\sigma\}$. The difference between the true stress field and the finite element stress field defines an *error stress field*:

$$\{\sigma_e\} = \{\sigma\} - \{\sigma_h\} \tag{1}$$

This error stress field may be integrated over the model to form the *strain energy of the error*:

$$U_e = \frac{1}{2}\int_V \{\sigma_e\}^T \{\varepsilon_e\}\, dV \tag{2}$$

where $\{\varepsilon_e\}$ are the elastic strains corresponding to $\{\sigma_e\}$ and V is the volume of the model.

In practice this integral is performed at the element level and the strain energy of the error (for the model) formed as the summation of elemental contributions. It is noted that for models for which the static boundary conditions are represented by consistent node forces, and for which the kinematic boundary conditions are homogeneous, the strain energy of the error is given directly as the difference between the true strain energy and the finite element strain energy:

$$U_e = U - U_h \tag{3}$$

Equation (3) states that the strain energy of the error is equal to the error of the strain energy.

The significance of the strain energy of the error can be determined by forming the *percentage error* with the true strain energy:

$$\alpha = \frac{U_e}{U} \times 100\% \tag{4}$$

The larger the value of α the more significant is the error in the model.

The development thus far has assumed that the true stress field $\{\sigma\}$ is known. Of course, in any practical situation the true solution will not be known and in order to proceed an estimate of the true stress field is required. The details of precisely how this is to be done will be discussed in the following section, however, assuming for the moment that an *estimated (true) stress field* $\{\tilde{\sigma}\}$[2] has been obtained, then an *estimated error stress field* can be defined as:

$$\{\tilde{\sigma}_e\} = \{\tilde{\sigma}\} - \{\sigma_h\} \tag{5}$$

The *strain energy of the estimated error* is formed in a similar way to the strain energy of the (true) error as:

$$\tilde{U}_e = \frac{1}{2}\int_V \{\tilde{\sigma}_e\}^T \{\tilde{\varepsilon}_e\}\, dV \tag{6}$$

where $\{\tilde{\varepsilon}_e\}$ are the elastic strains corresponding to $\{\tilde{\sigma}_e\}$.

[2]Note: the tilde will be used throughout to indicate estimated quantities.

The *estimated percentage error* is given as:

$$\tilde{\alpha} = \frac{\tilde{U}_e}{\tilde{U}} \times 100\% \qquad (7)$$

where $\tilde{U} = U_h + \tilde{U}_e$.

The parameter $\tilde{\alpha}$ is the error measure that can be used in a practical analysis to inform the engineer of the accuracy of the finite element solution. Elementwise distributions of $\tilde{\alpha}$ could be used in self-adaptive procedures to indicate areas of the model that required more (or indeed less) refinement for a specified level of accuracy.

The quality of the error measure is clearly dependent on the quality of the estimated stress field. Before one can confidently use any error estimator it must be tested on *benchmark problems* for which the (true) solution is known. The effectivity of an error estimator is formally quantified in terms of the *effectivity ratio*:

$$\beta = \frac{\tilde{U}_e}{U_e} \qquad (8)$$

The closer the effectivity ratio is to unity the more effective the error estimation. A desirable property of any error estimator is that as the mesh is refined the effectivity ratio tends to unity. Such a property is called asymptotic exactness. A good effectivity ratio (i.e. one that is close to unity) whilst indicating good error estimation in the sense of the definition of the effectivity ratio does not necessarily imply that the estimated stress field is a good approximation to the true one. Another integral quantity which measures the proximity of the estimated stress field to the true one is therefore defined. The *error in the estimated stress field* is defined as the difference between the true stress field and the estimated stress field:

$$\{\hat{\sigma}\} = \{\sigma\} - \{\tilde{\sigma}\} \qquad (9)$$

The *strain energy of the error in the estimated stress field* is then given as:

$$\hat{U} = \frac{1}{2}\int_V \{\hat{\sigma}\}^T \{\hat{\varepsilon}\} dV \qquad (10)$$

where $\{\hat{\varepsilon}\}$ are the elastic strains corresponding to $\{\hat{\sigma}\}$.

The smaller the value of this quantity, the closer the estimated stress field is to the true one.

CONTINUOUS ESTIMATED STRESS FIELDS

Before discussing estimated stress fields that are both continuous and boundary admissible, let us first review a number of available methods for obtaining estimated stress fields that are continuous. Procedures for achieving boundary admissibility will be discussed in the following section.

A standard method for achieving continuous stress fields is to interpolate from unique nodal stresses over each element with the element shape functions. The process of transforming a discontinuous finite element stress field into an estimated stress field that is continuous is shown diagramatically for a single component of stress and a patch of four elements in Fig. 1.

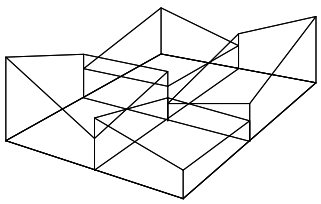

(a) Discontinuous σ_h

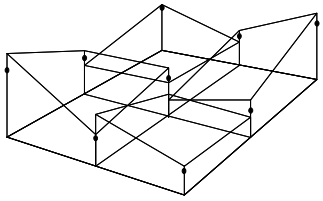

(b)Unique nodal stresses

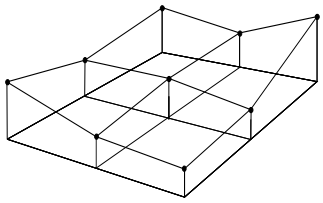

(c) Continuous $\tilde{\sigma}$

Fig. 1. Continuous $\tilde{\sigma}$ from discontinuous σ_h

The continuous estimated stress field $\{\tilde{\sigma}\}$ is defined, for each element, in terms of the shape functions for the element and a vector of unique nodal stresses $\{s\}$:

$$\{\tilde{\sigma}\} = [\overline{N}]\{s\} \tag{11}$$

where $[\overline{N}]$ is a matrix containing the shape functions for the element.

The vector $\{s\} = \lfloor \lfloor s \rfloor_1^T, \lfloor s \rfloor_2^T, \lfloor s \rfloor_3^T, \lfloor s \rfloor_4^T \rfloor^T$ where $\{s\}_i = \lfloor s_x, s_y, s_{xy} \rfloor^T$ is the vector of unique nodal stresses for node *i*.

Over recent years many methods for determining unique nodal stresses have been proposed. One might say that the method for obtaining unique nodal stresses is not in itself unique. Perhaps the simplest of all these methods is that of nodal averaging of the finite element stresses at a common node:

$$\{s\}_i = \frac{1}{n}\sum_{j=1}^{n} \{\sigma_h\}_i^j \tag{12}$$

where the summation is taken over the nodes of all elements *j* connected to node *i*.

Simple nodal averaging, as this technique is generally known, is commonly used in commercial finite element codes as a method for making the discontinuous finite element stresses more palatable to the engineer. The ANSYS suite of finite element software has included an error estimator based on a continuous estimated stress field derived from unique nodal stresses achieved through simple nodal averaging in its recent versions. The ANSYS error estimator, however, uses an inexact integration scheme known as nodal quadrature to perform the integration of the strain energy of the estimated error (equation (6)) and, although being commendably cheap in computational terms, this additional approximation results in an error estimator which is not asymptotically exact. Results demonstrating this point will be presented later in this paper (see Problem 3). Recent studies [15] have demonstrated that by using a slightly more costly, but exact, (at least for parallelogram shaped elements) integration scheme the property of asymptotic exactness can be recovered for the ANSYS error estimator.

Other methods of achieving sets of unique nodal stresses have concentrated on obtaining them through a least squares fit between the continuous estimated stress field and the finite element stress field [5,12]. However, although mathematically elegant, in addition to the high cost of obtaining the unique nodal stresses through global computations (c.f. simple nodal averaging where calculations are performed at a local, nodal level), the resulting error estimation has been demonstrated to be less effective than some that use simple nodal averaging [17].

More recently, the superconvergent patch recovery scheme of Zienkiewicz and Zhu [6] has received much attention. In this method the unique nodal stresses are obtained by interpolating from a stress surface fitted to the superconvergent stress points surrounding the node of interest. The fit is performed in a least squares manner individually for each component of stress. It has been claimed that this method results in high accuracy error estimation and that the nodal stresses thereby recovered are superconvergent. These claims have been investigated in [17] and the results are the subject of a paper shortly to be published [18].

The concept of a patch recovery scheme has been adopted by other researchers. For example Wiberg et al [7,20] employ a patch recovery scheme but, rather than perform the recovery individually for each component of stress as is done in the Zienkiewicz and Zhu approach, they do so for all components simultaneously. The coupling of the stress components is made through the equations of equilibrium.

Beckers, Zhong and Maunder have proposed a method of averaging and extrapolation for obtaining unique nodal stresses in a local manner [4]. This method bears strong similarities with the patch recovery scheme of Zienkiewicz and Zhu.

BOUNDARY ADMISSIBILITY

From a purely intuitive standpoint one might suggest that since the true stress field generally exhibits continuity then so an estimated stress field constructed from the finite element stress field such as to be continuous is likely to be a good candidate for the true stress field. One can reinforce this intuitive argument by considering that a continuous estimated stress field is also better than the original finite element stress field in that interface equilibrium is recovered i.e. some attempt is being made to recover the lost equilibrium. One can extend this idea further by requiring the estimated stress field to, in addition, satisfy the static boundary conditions. The idea of applying the static boundary conditions to an already continuous estimated stress field and thereby achieving a *continuous, boundary admissible estimated stress field* is discussed in this section.

The concept of modifying the *finite element stress field* with the known static boundary conditions is not new. Indeed, common sense tells us that where static boundary conditions are applied and, therefore, the direct stress normal to and the shear stress tangential to the surface are known we should disregard the finite element values and use values that are known to be true. Unfortunately, however, it is usually the third component of stress, the direct stress tangential to the surface, that is of interest to the engineer in any analysis. In an analogous fashion it makes sense to modify the *estimated stress field* with known values of stress. This idea has been used before in the improvement of the original finite element stress field $\{\sigma_h\}$ [13].

In [14] the importance of the static boundary conditions in achieving an asymptotically exact error estimator is discussed. Ways in which these boundary conditions can be applied to modify the continuous estimated stress field are now considered. All the ways aim to estimate the state of stress at nodes on the static boundary using original finite element stresses, and the specified boundary tractions, for patches of elements connected to the boundary nodes. Such a patch is illustrated in Fig. 2 for three methods: (a) a simple direct method as proposed in this paper [17], (b) that proposed by Mashaie [16] and (c) that proposed by Wiberg [20].

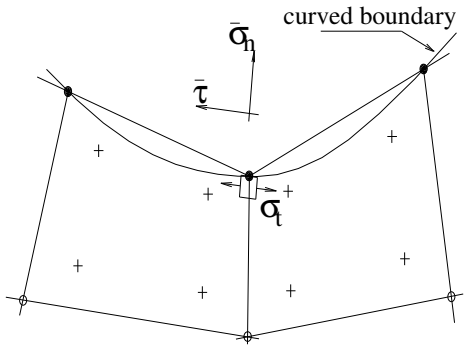

(a) Method proposed in this paper

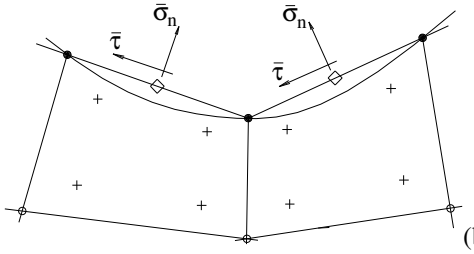

(b) Method proposed by Mashaie

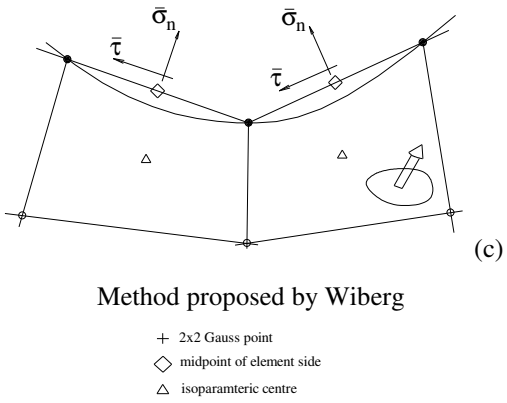

Fig. 2. Application of static boundary conditions on a smooth boundary

In the proposed method (a) the stress components σ_n and τ, which are normal and tangential to the boundary surface at the node, are equated to the specified tractions; the third component σ_t is determined by averaging nodal values in adjacent elements. As with internal nodes, the nodal values for an element are extrapolated from the four Gauss integration points using bilinear extrapolation functions. In method (b) three stages of stress averaging are involved. Nodal stresses are first determined as the average of the nearest Gauss point stresses. Stresses at the midpoints of the sides of elements which represent the boundary surface are then determined by averaging adjacent nodal stresses. These midpoint stresses are modified so that components σ_n and τ are equated to local values of the specified traction, and finally the nodal stresses are modified to be the average of adjacent midpoint stresses. Method (c) involves significantly more computation. The Superconvergent Patch Recovery concept [7] is extended to impose, in a weak sense, both internal equilibrium throughout the patch and boundary equilibrium at the two midpoints. The weak form of equilibrium is achieved by fitting a continuous stress field in a least squares sense to minimise weighted residuals in stress and body forces.

The examples considered in references [16,20] demonstrate that improvements can be achieved in error estimators through applying the static boundary conditions. The results presented in this paper using the simplified method of application, confirm the trends in improvements in comparison with the results of other error estimators currently under research. The details for the implementation of method (a) are now given with reference to Mesh 1 of Problem 2. This mesh is shown in detail in Fig.3.

For all nodes the first step in recovering the unique nodal stresses is to perform simple nodal averaging at each node. For internal nodes, such as node number 9, this is all the processing that is required. For boundary nodes, however, additional processing is necessary. For nodes that lie on a smooth boundary the direct stress normal to the surface σ_n and the shear stress tangential to the surface τ are defined. The remaining component of stress, the direct stress tangential to the surface σ_t, is generally unknown.

The unit vectors for node number 8 are shown in Fig. 3 normal (*n)* and tangential (*t)* to the actual boundary. The first step in the procedure for applying the static boundary conditions is to transform the nodal averaged stresses at the node of interest $\{s\}_i$ into the local, boundary co-ordinate system shown in Fig. 3. This requires a rotation of the stress components through an angle ϕ:

$$\{b\}_i = [R]\{s\}_i \tag{13}$$

where $[R] = \begin{bmatrix} \cos^2\phi & \sin^2\phi & \sin 2\phi \\ \sin^2\phi & \cos^2\phi & -\sin 2\phi \\ -\frac{1}{2}\sin 2\phi & \frac{1}{2}\sin 2\phi & \cos 2\phi \end{bmatrix}$

The nodal averaged stresses in the local, boundary co-ordinate system $\{b\}_i$ are now modified with the static boundary conditions:

$$\{\hat{b}\}_i = \begin{bmatrix} 0 & 0 & 0 \\ 0 & 1 & 0 \\ 0 & 0 & 0 \end{bmatrix} \{b\}_i + \begin{bmatrix} 1 & 0 & 0 \\ 0 & 0 & 0 \\ 0 & 0 & 1 \end{bmatrix} \begin{Bmatrix} \sigma_n \\ \sigma_t \\ \tau \end{Bmatrix} \quad (14)$$

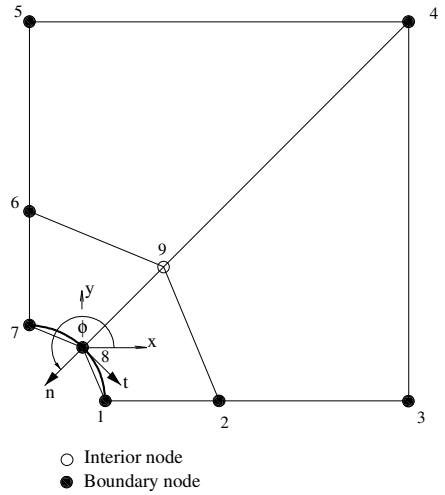

Fig. 3. Mesh 1 of Problem 2

Finally, the modified nodal averaged stresses $\{\hat{b}\}_i$ are transformed back into the global co-ordinate system:

$$\{\hat{s}\}_i = [R]^{-1} \{\hat{b}\}_i \quad (15)$$

For nodes that lie at the intersection of two orthogonal static boundaries e.g. node number 4 of Fig. 3, application of the static boundary conditions results in all three components of stress being modified to known true values. For nodes that lie completely on symmetry boundaries e.g. node numbers 2 & 6 of Fig. 3, the only known condition on the stresses is that the shear stress tangential to the surface is zero i.e. $\tau = 0$. Node numbers 1,3,5 & 7 lie at the intersection of static and symmetric boundaries. For these nodes the symmetry condition is automatically satisfied by modifying according to the static boundary conditions on the static boundary.

This method can easily be extended to cover the more general case of a boundary surface with convex or concave corners, where normal and tangential directions are not uniquely defined. These cases are illustrated in Fig. 4. In reality such corners will have radii, albeit with small values. However, finite element models composed of four-noded straight sided elements cannot represent exactly general curved boundaries, let alone corner radii with possibly uncertain values. This is only really of concern if stress distributions are sought in the neighbourhood of corners. Otherwise it is common to represent a corner by the node at the intersection of two sides.

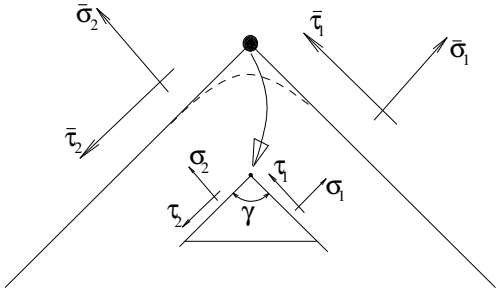

(a)

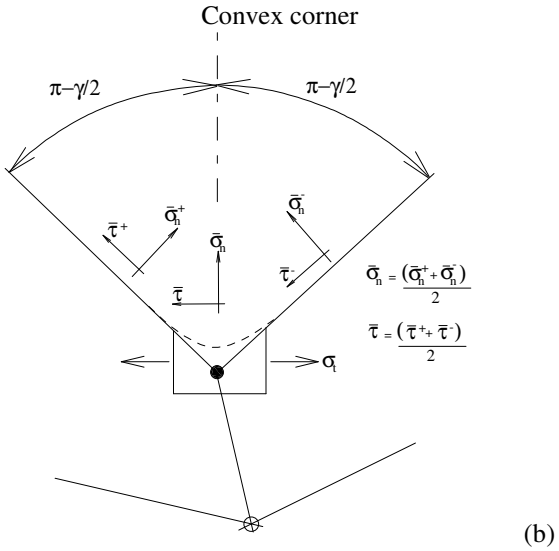

(b)

Fig. 4. Application of static boundary conditions on a polygonal boundary

Fig. 4(a) shows a convex corner with four specified components of traction adjacent to the corner node. If the components are consistent with a unique state of stress within the corner, then this stress is imposed at the node. If the components are inconsistent, then a unique nodal stress can be defined from consistent components σ_1, τ_1, σ_2, τ_2 defined so that:

$$(\sigma_1-\overline{\sigma}_1)^2+(\tau_1-\overline{\tau}_1)^2+(\sigma_2-\overline{\sigma}_2)^2+(\tau_2-\overline{\tau}_2)^2 \quad (16)$$

is minimised subject to:

$$(\tau_1+\tau_2)=(\sigma_1-\sigma_2)\cot\gamma \quad (17)$$

which is the consistency condition for a unique state of stress.

In this case:

$$\begin{Bmatrix}\sigma_1\\ \tau_1\\ \sigma_2\\ \tau_2\end{Bmatrix}=\begin{Bmatrix}\overline{\sigma}_1\\ \overline{\tau}_1\\ \overline{\sigma}_2\\ \overline{\tau}_2\end{Bmatrix}-e\frac{\sin\gamma}{2}\begin{Bmatrix}-\cos\gamma\\ \sin\gamma\\ \cos\gamma\\ \sin\gamma\end{Bmatrix} \quad (18)$$

where $e=\left[\overline{\tau}_1+\overline{\tau}_1-(\overline{\sigma}_1-\overline{\sigma}_2)\cot\gamma\right]\neq 0$.

Fig. 4(b) shows a concave (re-entrant) corner with normal and tangential tractions which may be specified with discontinuities at the corner node. In this case average values are assumed in the directions of the bisector of the corner angle, and perpendicular to this bisector. The stress components at the corner node are taken as the average traction values $\overline{\sigma}_n$ and $\overline{\tau}$, and σ_t is averaged as in the case of a smooth boundary surface as illustrated in Fig. 2(a).

ERROR ESTIMATORS INVESTIGATED

In the following sections the performance of a number of error estimators using continuous and continuous, boundary admissible estimated stress fields will be investigated. However, before doing this it is necessary to formally define the error estimators that will be examined.

Two error estimators will be examined. Both use continuous estimated stress fields as defined by equation (11). The first error estimator EE_2 (the subscript 2 is used in order to retain a consistency with previously published work e.g. [15]) uses unique nodal stresses obtained by a process of simple nodal averaging. The second error estimator EE_2^b is identical to EE_2 in all respects except that the estimated stress field in addition to being continuous is also boundary admissible. Boundary admissibility is achieved by modifying all values of nodal stress affected by the static boundary conditions to the known, true values using the simple direct method detailed in this paper. Comparison of the two error estimators (EE_2 and EE_2^b) will be made on the basis of the effectivity ratio of equation (8) (β_2 and β_2^b respectively for the two error estimators) and on the strain energy of the error of the estimated stress field of equation (10) ($\widehat{U}_2$ and $\widehat{U}_2^b$ respectively for the two error estimators).

In addition to the two error estimators EE_2 and EE_2^b, for the third problem presented in this paper the effectivity ratios of a number of other error estimators using continuous estimated stress fields will also be reported. These error estimators are:

EE_p: This error estimator uses unique nodal stresses recovered from a patch recovery scheme. The parent patch recovery scheme of reference [19] is used here.

EE_{ZZ}: This error estimator is the original Zienkiewicz and Zhu error estimator proposed in [5] and uses unique nodal stresses recovered from a global least squares fit between the continuous estimated stress field and the finite element stress field[3].

EE_4: This error estimator is the one used in the ANSYS suite of finite element software and has been discussed in detail in reference [15].

NUMERICAL EXAMPLES

In order to demonstrate the improved effectivity of error estimators using continuous, boundary admissible estimated stress fields over those that simply use a

[3]The results for this error estimator have been taken from reference [4].

continuous estimated stress field, four numerical examples will be presented. The problems investigated, although perhaps chosen in an arbitrary fashion, are realistic problems exhibiting characteristics with which a practising engineer is likely to be familiar. All problems are force driven with a plane stress constitutive relationship. The only conditions placed on the displacements are those necessary to eliminate rigid body motions.

Problem 1. This problem involves a rectangular membrane loaded with static boundary conditions consistent with the linear statically and kinematically admissible stress field generally associated with a beam under pure (engineer's) bending. The true stress field for this problem is:

$$\begin{aligned} \sigma_x &= 30\,y \\ \sigma_y &= 0 \\ \tau_{xy} &= 0 \end{aligned} \qquad (19)$$

and has been plotted in Fig. 8(a).

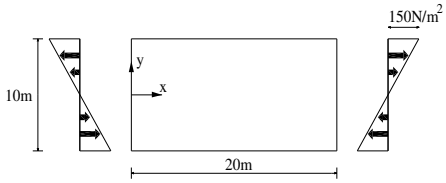

Fig. 5. Geometry of Problem 1

For a Young's Modulus of $E = 210\,N/m^2$, a Poisson's Ratio of $\nu = 0.3$ and a material thickness of $t = 0.1m$, the strain energy for the problem is:

$$U = \frac{2500}{7} \approx 357.14\,Nm \qquad (20)$$

This problem has also been reported in [15,17,19]. The geometry and static boundary conditions are shown in Fig. 5.

The way in which an error estimator performs with coarse and, possibly, distorted meshes is of interest to an engineer. This problem investigates the performance of the error estimators as a coarse, but regular mesh is progressively distorted. The meshes that will be used in the problem are shown in Fig. 6.

Table 1. Results for Problem 1

Mesh	β_2	β_2^b	$\widehat{U}_2$	$\widehat{U}_2^b$
1	0.71	0.82	103.7	7.7
2	0.60	0.81	114.7	20.3
3	0.37	0.81	146.6	54.3
4	0.20	0.82	196.7	100.5
5	0.13	0.81	272.1	147.3

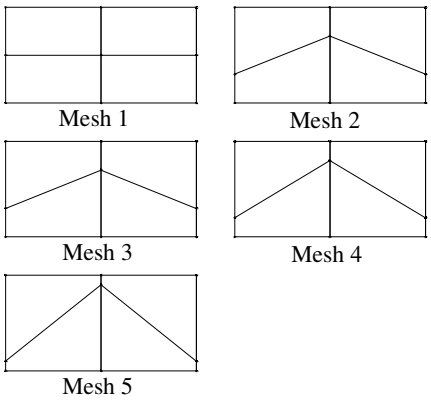

Fig. 6. Meshes for Problem 1

The effectivity ratio and the strain energy of the error of the estimated stress are tabulated in Table 1 and the variation of effectivity ratio with distortion is shown in Fig. 7. The stress fields for Mesh 1 are illustrated in Figure 8.

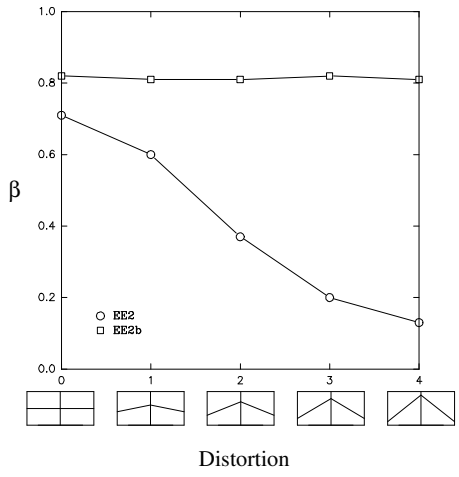

Fig. 7. β versus distortion for Problem 1

Problem 2. This problem involves a square membrane with a central circular hole of radius a and is the classical problem of a stress concentration in an infinite membrane. The true stress field for this problem is:

$$\sigma_x = \sigma_\infty \{1 - \frac{a^2}{r^2}(\frac{3}{2}\cos 2\theta + \cos 4\theta) + \frac{3}{2}\frac{a^4}{r^4}\cos 4\theta\}$$
$$\sigma_y = \sigma_\infty \{0 - \frac{a^2}{r^2}(\frac{1}{2}\cos 2\theta - \cos 4\theta) - \frac{3}{2}\frac{a^4}{r^4}\cos 4\theta\} \quad (21)$$
$$\tau_{xy} = \sigma_\infty \{0 - \frac{a^2}{r^2}(\frac{1}{2}\sin 2\theta + \sin 4\theta) + \frac{3}{2}\frac{a^4}{r^4}\sin 4\theta\}$$

where σ_∞ is the value of σ_x at $x = \pm\infty$ and is chosen as $10,000\ N/m^2$ for this problem. This stress field has been taken from reference [3].

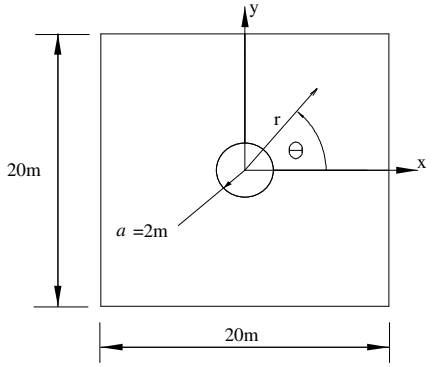

Fig. 9. Geometry of Problem 2

The finite portion of this infinite membrane shown in Fig. 9 will be modelled. Static boundary conditions are determined from the stress field given above. Through the symmetry present in this problem only one quarter of the membrane need be modelled and the four meshes, of increasing refinement, that will be used are shown in Fig. 10.

For a Young's Modulus of $E = 10 \times 10^6\ N/m^2$, a Poisson's Ratio of $\nu = 0.25$ and a material thickness of $t = 0.01m$ the strain energy for this problem is:

$$U = 5.188448459\,Nm \quad (22)$$

and is accurate to the number of digits quoted [17].

This problem has also been reported in [17,18].

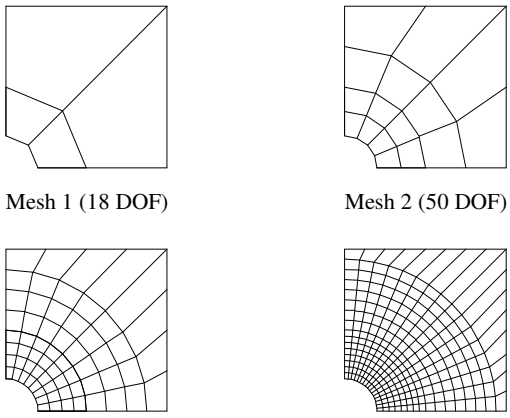

Fig. 10. Meshes for Problem 2

The results for Problem 2 are tabulated in Table 2 and the convergence of the effectivity ratios with number of degrees of freedom are plotted in Fig. 11.

Table 2.Results for Problem 2

Mesh	β_2	β_2^b	$\widehat{U}_2$	$\widehat{U}_2^b$
1	0.2768	0.8766	0.1498	0.1590
2	0.4456	1.1349	0.0469	0.0459
3	0.5855	1.0429	0.0115	0.0078
4	0.7054	0.9309	0.0023	0.0009

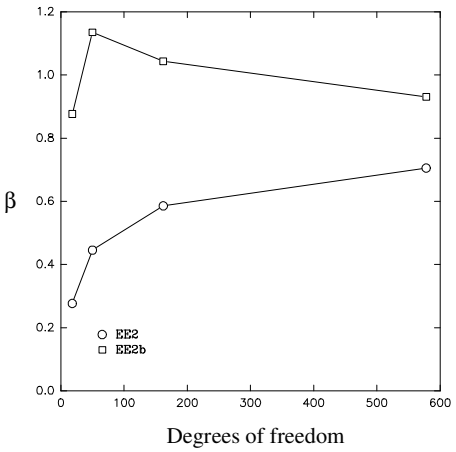

Fig. 11. β versus DOF for Problem 2

Problem 3. This problem involves a rectangular membrane loaded with static boundary conditions

consistent with the quadratic statically and kinematically admissible stress field typically associated with a simply supported beam under the action of a transverse shear force. The true stress field for this problem is:

$$\begin{aligned}\sigma_x &= 46.875xy \\ \sigma_y &= 0 \\ \tau_{xy} &= 93.75 - 23.4375y^2\end{aligned} \qquad (23)$$

For a Young's Modulus of $E = 3\times10^7\ N/m^2$, a Poisson's Ratio of $\nu = 0.3$ and a material thickness of $t = 1m$, the strain energy for the problem is:

$$U = \frac{239}{6000} \approx 0.03983'\ Nm \qquad (24)$$

This problem has also been reported in [4,17].

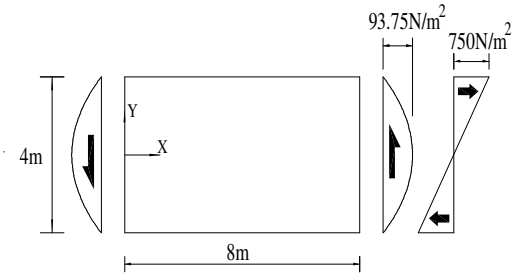

Fig. 12. Geometry of Problem 3

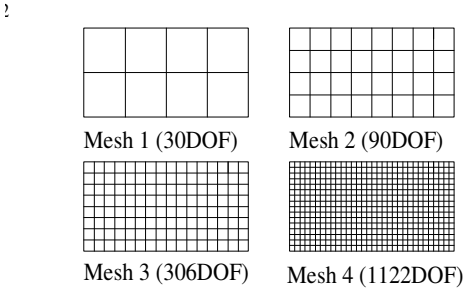

Fig. 13. Meshes for Problem 3

Whereas Problem 1 dealt with the performance of error estimators with coarse and distorted meshes, this problem looks at how the error estimators perform as a mesh is refined. The geometry and static boundary conditions for Problem 3 are shown in Fig. 12 and the meshes that are used are shown in Fig. 13. The convergence of the effectivity ratios with number of degrees of freedom are plotted in Fig. 14.

Table 3. Results for Problem 3

Mesh	1	2	3	4
β_2	0.7120	0.9270	0.9804	0.9947
β_2^b	1.0887	1.0518	1.0188	1.0062
$\widehat{U}_2$	375e-5	66e-5	9.43e-5	1.25e-5
$\widehat{U}_2^b$	171e-5	20e-5	1.68e-5	0.13e-5
β_p	0.7450	0.9442	0.9853	0.9960
β_{ZZ}	(i)	0.81	0.90	0.96
β_4	1.76	2.28	2.60	2.79

(i) The result for this error estimators and this mesh was not available in [4].
(ii) The effectivity ratios β_p, β_{ZZ} and β_4 correspond to the error estimators EE_p, EE_{ZZ} and EE_4 defined in the section 'Error Estimators Investigated'.

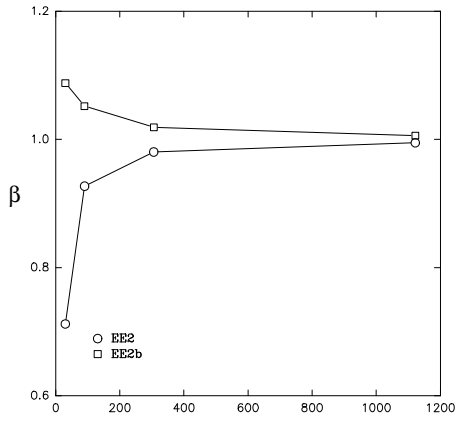

Fig. 14. β versus DOF for Problem 3

Problem 4. This problem involves a rectangular membrane with an infinitesimally thin crack of length $5m$ as shown in Fig. 15. The true stress field for this problem is:

$$\begin{aligned}\sigma_x &= \frac{100}{\sqrt{r}}\cos\frac{\theta}{2}\{1-\sin\frac{\theta}{2}\sin\frac{3\theta}{2}\} \\ \sigma_y &= \frac{100}{\sqrt{r}}\cos\frac{\theta}{2}\{1+\sin\frac{\theta}{2}\sin\frac{3\theta}{2}\} \\ \tau_{xy} &= \frac{100}{\sqrt{r}}\sin\frac{\theta}{2}\cos\frac{\theta}{2}\cos\frac{3\theta}{2}\end{aligned} \qquad (25)$$

and is taken from reference [3].

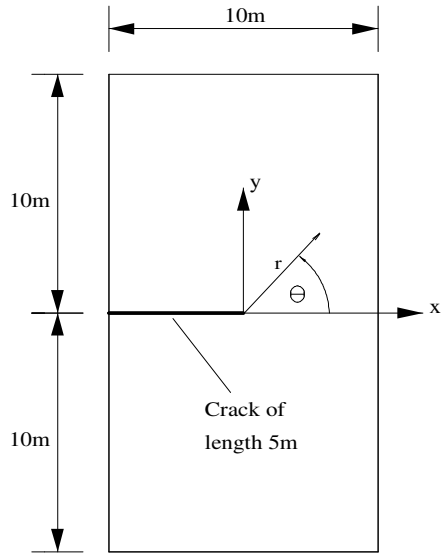

Fig. 15. Geometry of Problem 4

For a Young's Modulus of $E = 210\, N/m^2$, a Poisson's Ratio of $\nu = 0.3$ and a material thickness of $t = 0.1m$ the strain energy for this problem is:

$$U = 124.885926020\, Nm \qquad (26)$$

and is accurate to the number of figures quoted [17].

Static boundary conditions are determined from the stress field given in equation (25) and are applied to the four meshes shown in Fig. 16.

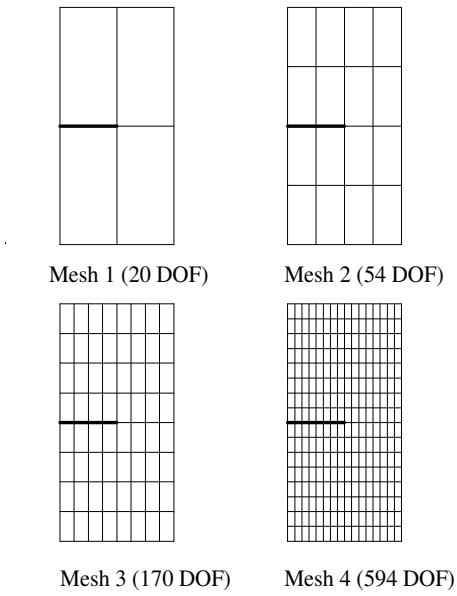

Fig. 16. Meshes for Problem 4

The results for Problem 4 are tabulated in Table 4 and the convergence of the effectivity ratios with number of degrees of freedom are plotted in Fig. 17.

Table 4.Results for Problem 4

Mesh	β_2	β_2^b	$\widehat{U}_2$	$\widehat{U}_2^b$
1	0.23	0.53	32.38	28.56
2	0.45	0.64	19.01	17.99
3	0.51	0.73	10.36	9.95
4	0.57	0.81	5.33	5.04

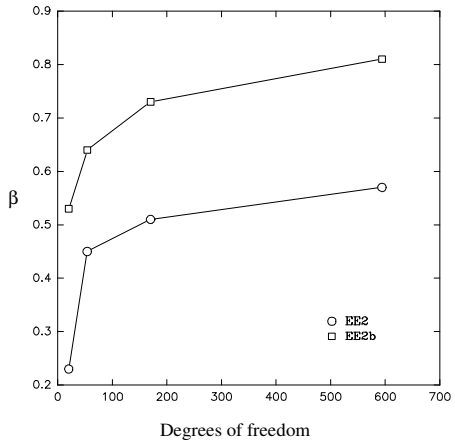

Fig. 17. β versus DOF for Problem 4

DISCUSSION AND CONCLUSIONS

This paper has presented a simple error estimator (EE_2^b) for the four-noded Lagrangian quadrilateral element in which a continuous, boundary admissible estimated stress field is used. Unique nodal stresses achieved by simple nodal averaging for which the components defined by the static boundary conditions have been corrected to the true values are interpolated over each element with the finite element shape functions. The effectivity of this error estimator is then compared with that of one which does not take account of the static boundary conditions (EE_2). The basis for comparison is made on the effectivity ratio β, and the strain energy of the error in the estimated stress field $\widehat{U}$. The effectivity ratio measures the proximity of the

strain energy of the estimated error with that of the true error in the form of a ratio whilst $\widehat{U}$ measures the proximity of the estimated stress field to the true one. For effective error estimation one requires an effectivity ratio that is close to unity and, further, it is desirable that the effectivity ratio tends to unity as the mesh is refined i.e. that it is asymptotically exact. Recognising that the effectivity ratio says little about the pointwise quality of the estimated stress field leads to the introduction of the quantity $\widehat{U}$. This quantity is an absolute value; small values indicating good pointwise quality of the estimated stress field.

The two error estimators, EE_2 and EE_2^b, have been tested on four problems that should be familiar to practising engineers. Problem 1 looks at how the error estimators are affected by element distortion for a fairly coarse mesh. This is important because it is in precisely these types of situation that one would like to achieve good error estimation. Problem 2 looks at how the error estimators perform with mesh refinement for a problem involving a stress concentration. Problem 3 looks at how the error estimators perform with mesh refinement for a problem involving a smooth solution but one which is one degree higher than the element is capable of modelling. For this problem the effectivities of a number of other error estimators are reported for comparison. Finally, Problem 4 shows how the error estimators perform in the presence of a singularity in stress.

For all four problems it is clearly seen that the simple expedient of applying the static boundary conditions to the estimated stress field results in higher quality error estimation. This is evidenced by the fact that β_2^b is closer to unity than β_2 and that $\widehat{U}_2^b$ is always close to and is generally less than $\widehat{U}_2$.

For Problem 1, where the effectivity of EE_2 is strongly affected by the level of distortion (see Fig. 7), it is seen that application of the static boundary conditions leads to an error estimator EE_2^b that is virtually unaffected by the level of distortion present in the mesh. The process of transforming the finite element stress field into one which is continuous and then into one which is continuous and boundary admissible is shown for Problem 1 in Fig 8(b,c and d). The improvement in the pointwise quality of the estimated stress field through application of the static boundary conditions is clearly seen in this figure and is reflected in the value of $\widehat{U}_2^b$ when compared with that of $\widehat{U}_2$.

For Problem 2 similar improvements are also noted with EE_2^b providing significantly more effective error estimation than EE_2. Note, with respect to this problem, that β_2^b appears to be converging but not monotonically. The reason for this is felt to lie in the coarseness of the approximation of Mesh 1 both in terms of the mesh discretisation and in terms of the geometry; the circular arc is being approximated by two lines. This mesh also produces a situation where, whilst being close to each other, $\widehat{U}_2^b$ is greater than $\widehat{U}_2$.

For Problem 3 similar improvements in the quality of the error estimation observed for the previous two problems are also noted. It is interesting to observe, for this problem, that β_2^b is always greater than unity. This, in turn, implies that the strain energy of the estimated error is greater than that of the true error. This 'upper bound' type of behaviour is typical for error estimators that use statically admissible estimated stress fields (see reference [10] for example). However, although the estimated stress field of EE_2^b does satisfy equilibrium on element interfaces and at the static boundary of the model, nothing has been done to enforce internal equilibrium and, as such, in general one cannot expect this upper bound type of behaviour. Indeed, for Problem 1 and for Mesh 1 of Problem 2, β_2^b is less than unity.

For Problem 3 the effectivity ratios for a number of other error estimators are presented. These are discussed in order of appearance in Table 3. Error estimator EE_p is a modified version of the error estimator proposed by Zienkiewicz and Zhu in which the unique nodal stresses are recovered using a patch recovery scheme [6]. The modification that has been applied takes the form of a re-definition of the co-ordinate system in which the patch is defined (see reference [19]) and has been made to overcome the problem of ill-conditioning (and possible singularity) of the equations used to recover the unique nodal stress whilst using the bi-linear form of the stress surface recommended in [6]. The performance of this error estimator is comparable, and slightly better than that of EE_2. It is, however, significantly less effective than EE_2^b. Recent studies [17] have demonstrated that similar improvements in effectivity by applying the static boundary conditions, here demonstrated for an error estimator using simple nodal averaging as a means for determining unique nodal stresses, can also be achieved when using a patch recovery scheme for achieving unique nodal stresses.

Error estimator EE_{ZZ} is the original error estimator proposed by Zienkiewicz and Zhu in their 1987 paper [5] and uses a global least squares fit between the continuous estimated stress field and the finite element stress field as a means of obtaining unique nodal stresses. This error estimator is significantly more costly than the other ones detailed in this paper due to the fact that the computations required to recover the unique nodal stresses are performed at the global level (i.e. for the whole model simultaneously) rather than at the element or nodal level. The performance of this error estimator can be seen (c.f. Table 3) to be not as good as those that use the cheaper, local computations i.e. EE_2, EE_2^b and EE_p.

Finally, results for the error estimator EE_4 have also been reported. This error estimator is similar to EE_2 in that it uses simple nodal averaging to achieve the unique nodal stresses. However, it differs in two significant ways. Firstly, for elements involving nodes that are attached to only a single element, a modification factor is applied to take account of the fact that no error is detected at such nodes (the nodal averaged values of stress are identical to the finite element values). Details of this correction factor can be found in reference [15]. Secondly, and more significantly the way in which the integration of the strain energy of the estimated error is performed is different. Whereas in all other error estimators detailed in this paper this quantity is integrated using the appropriate Gauss quadrature scheme i.e. using a 2x2 scheme yields exact integration for undistorted (parallelogram shaped) elements, EE_4 uses a method of integration, termed nodal quadrature, which is approximate even for undistorted elements. It has been shown [15] that the nature of this approximation is such that the strain energy of the estimated error achieved in this manner is always greater than that which would have been achieved using an appropriate Gauss quadrature scheme. This leads to the very high effectivity ratios detailed in Table 3 and gives an explanation for the lack of asymptotic exactness exhibited by this error estimator.

The singularity in stress makes Problem 4 a challenging one for the element under consideration. However, even with such poor finite element approximation the enhancement in quality of error estimation obtained by applying the static boundary conditions is dramatic c.f. Fig. 17.

In conclusion, this paper has attempted to demonstrate the increased effectivity of error estimators that can be achieved by the simple expedient of applying the static boundary conditions to the estimated stress field. This

increase in effectivity is significant especially for coarse and distorted meshes where effective error estimation is most called for. With the current trend in pre- and post-processors being such that geometrical and boundary condition information is available after completion of the analysis stage, it is a relatively simple task to code this facility into existing finite element software. However, it should be noted that the studies presented in this paper pertain to a particular element type, namely, to the standard four-noded Lagrangian displacement element. The extension to higher order elements such as the eight-noded serendipity element is not (as has often been surmised) straight forward for it is well known, and has been widely reported [4] that for the eight-noded element consideration of lack of interface equilibrium alone is insufficient to provide effective error estimation.

REFERENCES

1. I. Babuska and W. C. Rheinbolt, *A posteriori* error estimates for the finite element method, Int. J. Numer. Meth. Engng. **12**, 1597-1615, (1978).

2. D. W. Kelly, J. P. Gago, O. C. Zienkiewicz and I. Babuška, *A posteriori* error analysis and adaptive processes in the finite element method: Part I-Error analysis, Int. J. Numer. Meth. Engng. **19**, 1593-1619 (1983).

3. B. Szabó and I. Babuška, Finite element analysis, John Wiley & Sons, (1991).

4. P. Beckers, H. G. Zhong and E. A. W. Maunder, Numerical comparison of several *a posteriori* error estimators for 2D stress analysis, Revue Européene des Élements Finis, 2(2), 155-178, (1993).

5. O. C. Zienkiewicz and J. Z. Zhu, A simple error estimator and adaptive procedure for practical engineering analysis, Int. J. Numer. Meth. Engng. **24**, 337-357, (1987).

6. O. C. Zienkiewicz and J. Z. Zhu Superconvergent derivative recovery techniques and *a posteriori* error estimation in the finite element method Part I: A general superconvergent recovery technique, Int. J. Numer. Meth. Engng. **33**, 1331-1364 (1992).

7. N. E. Wiberg and F. Abdulwahab Patch recovery based on superconvergent derivatives and equilibrium, Int. J. Numer. Meth. Engng. **36**, 2703-2724 (1993).

8. P. Ladevèze and D. Leguillon, Error estimate procedure in the finite element method and applications', SIAM J. Numer. Anal. 20 (No. 3), 483-509 (1983).

9. H. Ohtsubo and M. Kitamura, Element by element *a posteriori* error estimation and improvement of stress solutions for two-dimensional elastic problems, Int. J. Numer. Meth. Engng. **29**, 233-244, (1990).

10. E. A. W. Maunder and W. G. Hill, Complementary use of displacement and equilibrium models in analysis and design, Proceedings of the sixth World Congress on Finite Element Methods, Banff, (1990).

11. J. D. Yang, D. W. Kelly and J. D. Isles, *A posteriori* pointwise upper bound error estimates in the finite element method, Int. J. Numer. Meth. Engng. **36**, 1279-1298 (1993).

12. E. Hinton and J. S. Campbell, Local and global smoothing of discontinuous finite element functions using a least squares method, Int. J. Numer. Meth. Engng. **8**, 461-480, (1974).

13. G. Cantin, G. Lobignac and G. Touzot, An iterative algorithm to build continuous stress and displacement solutions, Int. J. Numer. Meth. Engng. **12**, 1439-1506, (1978).

14. M. Ainsworth, J. Z. Zhu, A. W. Craig and O. C. Zienkiewicz, Analysis of the Zienkiewicz-Zhu *a posteriori* error estimator in the finite element method, Int. J. Numer. Meth. Engng. **28**, 2161-2174 (1989).

15. J. Robinson, E. A. W. Maunder and A. C. A. Ramsay, Some studies of simple error estimators, FEN, Issues 4, 5 and 6, (1992) and Issues 1, 2 and 3, (1993).

16. A. Mashaie, E. Hughes and J. Goldak, Error estimates for finite element solutions of elliptic boundary value problems, Comput. Struct. **49**(1), 187-198, (1993).

17. A. C. A. Ramsay, Finite element shape sensitivity and error measures, Ph. D. Thesis, University of Exeter (1994).

18. A. C. A. Ramsay and H. Sbresny, Evaluation of some error estimators for the four-noded Lagrangian quadrilateral, Accepted for publication in Comm. Numer. Meth. Engng, (1995).

19. A. C. A. Ramsay and H. Sbresny, Some studies of an error estimator based on a patch recovery scheme, FEN, Issues 2 and 4 (1994).

20. N. E. Wiberg, F. Abdulwahab and S. Ziukas, Enhanced superconvergent patch recovery incorperating equilibrium and boundary conditions, Int. J. Numer. Meth. Engng. **37**, 3417-3440, (1994).

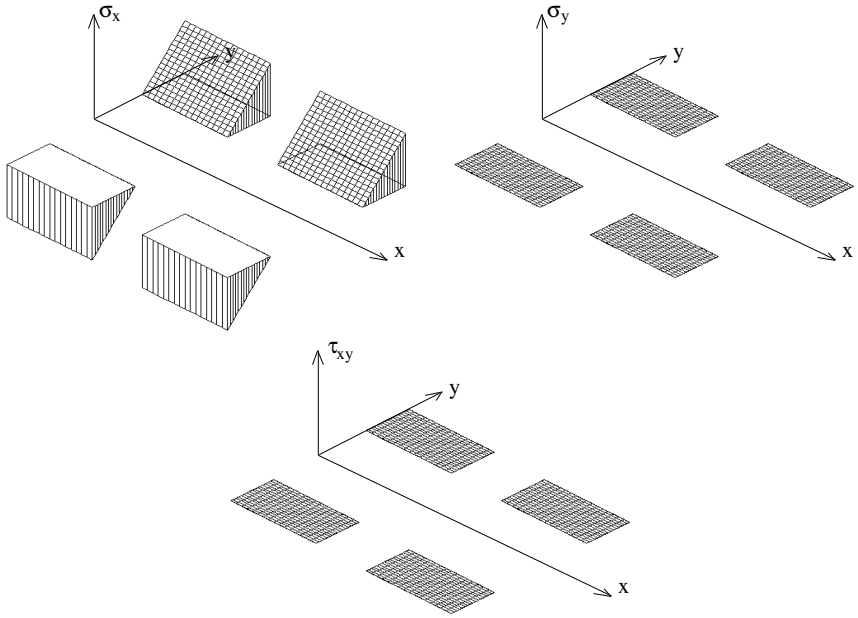

(a) True stress field $\{\sigma\}$

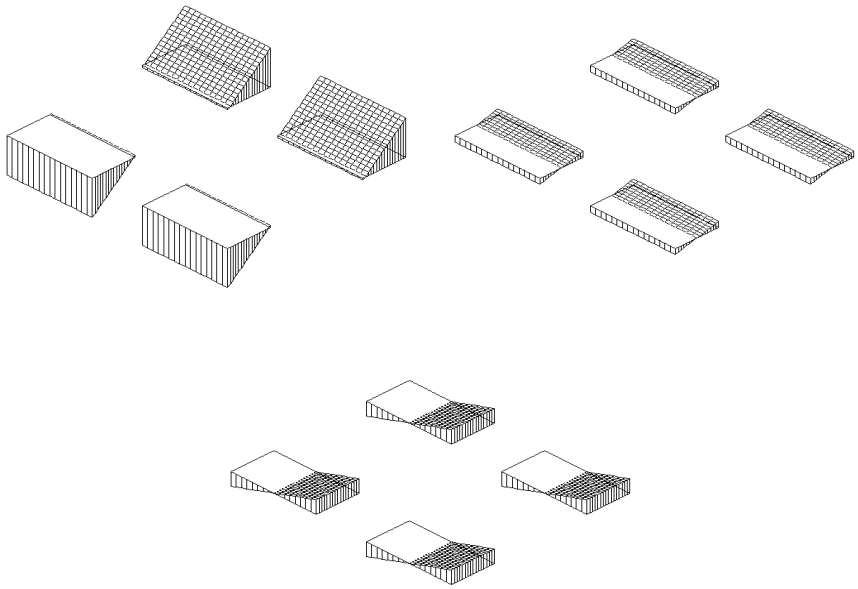

(b) Finite element stress field $\{\sigma_h\}$

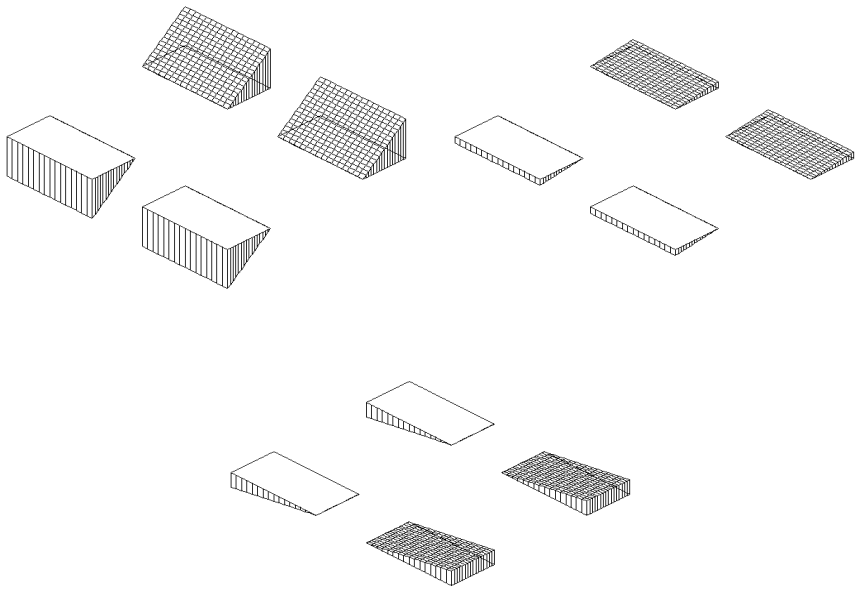

(c) Continuous estimated stress field of EE_2 ($\beta_2 = 0.71,\ \widehat{U}_2 = 103.7$)

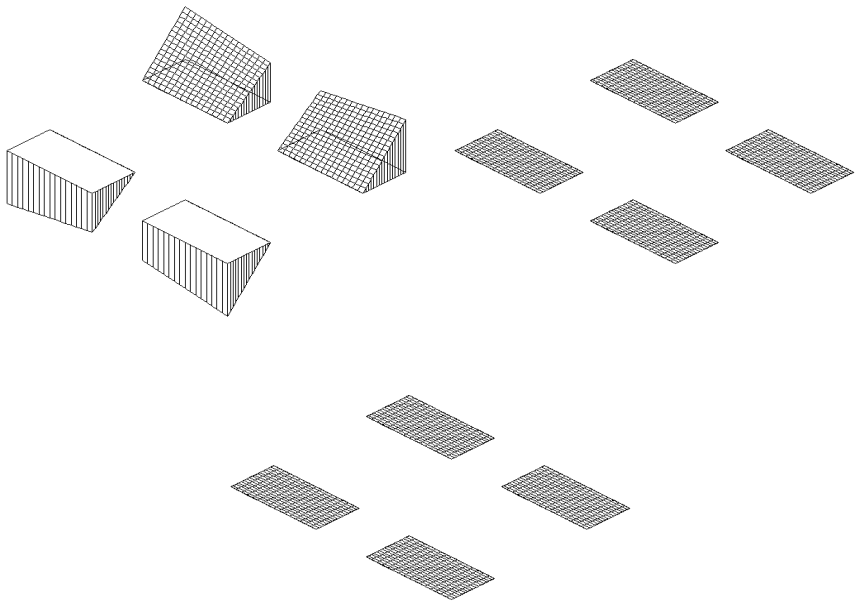

(d) Continuous, boundary admissible estimated stress field of EE_2^b ($\beta_2^b = 0.82,\ \widehat{U}_2^b = 7.7$)

Fig. 8. Stress fields for Problem 1